

Relationship between the Dipole Strength of Ligand Pre-Edge Transitions and Metal–Ligand Covalency

Frank Neese, Britt Hedman, Keith O. Hodgson, and Edward I. Solomon*

Department of Chemistry and Stanford Synchrotron Radiation Laboratory, Stanford University, Stanford, California 94305

Received April 29, 1999

The electric dipole contributions to the observed pre-edge intensities in ligand K-edge X-ray absorption (XAS) spectra are analyzed in terms of covalent-bonding contributions between the metal and ligand for a prototype system with one hole in the d shell. One- and two-center contributions to the intensity are identified. By direct evaluation of the integrals involved in the intensity expression, the two-center terms are shown to be at least 1 order of magnitude smaller than the one-center terms and can be ignored to a reasonable approximation. The one-center terms reflect the amount of ligand character in the partially occupied metal-based MOs and are proportional to the intrinsic transition moment of a ligand-centered $1s \rightarrow np$ transition. The final intensity does not contain terms proportional to the square of the metal–ligand distance as might have been expected on the basis of the analogy between ligand K-edge and ligand-to-metal charge transfer (LMCT) transitions that both formally lead to transfer of electron density from the ligand to the metal. This is due to the fact that the transition density is completely localized on the ligand in the case of a ligand K-edge transition but is delocalized over the metal and the ligand in the case of a LMCT transition. The effective nuclear charge dependence of the one-center transition moment integral was studied by Hartree–Fock level calculations and was found to be small. Electronic relaxation effects were considered and found to be small from a Hartree–Fock calculation on a cupric chloride model.

Introduction

Covalent bonding between open-shell transition metal ions and their ligands plays a key role in the formation of inorganic compounds and determining their reactivities. The covalency of the metal–ligand bonds is in many ways related to the chemistry of the complexes.¹ For example, covalent bonds imply large charge donation to the central metal which ultimately lowers the redox potential of the $M^{n+}/M^{(n-1)+}$ couple. Covalent bonding of bridging ligands is effective in mediating antiferromagnetic coupling via superexchange pathways.^{2–8} Furthermore anisotropy in the covalent bonding is believed to facilitate directional long-range electron transfer.^{9–12} It is therefore of utmost importance to quantitatively define metal–ligand covalency on both an experimental and a theoretical level.

The effects of covalent bonding are particularly prominent in the molecular spectra of transition metal complexes. However, when it comes to the estimation of covalencies from experimental data, some qualification is necessary of what is actually measured. In general, experiments based on magnetic resonance techniques measure the spin density of the ground state while optical experiments probe the transition densities between the ground state and a given excited state in the spectral region of interest.^{13,14} If, within the restrictions imposed by the MO method, the same MOs describe the ground and excited states (i.e., no electronic relaxation), the ground state mixing ratios between the metal and ligand orbitals within the partially occupied MOs can in both cases approximately be related to experimental observables and are commonly reported as percentages of mixing of ligand into metal orbitals. However, it must be remarked that covalency in a spectroscopic sense is related not only to metal–ligand orbital mixing ratios (the “symmetry-restricted covalency”^{15–18}) but also to the distortions of the metal orbitals upon bond formation (the “central-field covalence”;^{15–18} for a recent discussion, see ref 19). It is clear that the division of either the spin density or the transition density into metal- and ligand-centered parts is always to a

* To whom correspondence should be addressed at the Department of Chemistry.

- (1) Holm, R. H.; Kennepohl, P.; Solomon, E. I. *Chem. Rev.* **1996**, *96*, 2239.
- (2) Anderson, P. W. *Phys. Rev.* **1959**, *115*, 2.
- (3) Kahn, O. *Molecular Magnetism*; VCH Publishers: New York, 1993.
- (4) Bencini, A.; Gatteschi, D. *EPR of Exchange Coupled Systems*; Springer: Heidelberg, Germany, 1990.
- (5) Ross, P. K.; Allendorf, M. D.; Solomon, E. I. *J. Am. Chem. Soc.* **1989**, *111*, 4009.
- (6) Tuzcek, F.; Solomon, E. I. *Inorg. Chem.* **1993**, *32*, 2850.
- (7) Gamelin, D. R.; Bominaar, E. L.; Kirk, M. L.; Wieghardt, K.; Solomon, E. I. *J. Am. Chem. Soc.* **1996**, *118*, 8085.
- (8) Gamelin, D. R.; Bominaar, E. L.; Mathoniere, C.; Kirk, M. L.; Wieghardt, K.; Girerd, J.-J.; Solomon, E. I. *Inorg. Chem.* **1996**, *35*, 4323.
- (9) Solomon, E. I. *Comments Inorg. Chem.* **1984**, *3*, 227.
- (10) Solomon, E. I.; Baldwin, M. J.; Lowery, M. D. *Chem. Rev.* **1992**, *92*, 521.
- (11) Solomon, E. I.; Lowery, M. D. *Science* **1993**, *259*, 1575.
- (12) Newton, M. D. *Chem. Rev.* **1991**, *91*, 767.

- (13) McWeeny, R. *Spins in Chemistry*; Academic Press: New York, London, 1970.
- (14) McWeeny, R. *Methods of Molecular Quantum Mechanics*; Academic Press: London, San Diego, New York, Boston, Sydney, Tokyo, Toronto, 1992.
- (15) Jørgensen, C. K. *Orbitals in Atoms and Molecules*; Academic Press: London, New York, 1962.
- (16) Jørgensen, C. K. *Adv. Chem. Phys.* **1963**, *33*.
- (17) Jørgensen, C. K. *Struct. Bonding* **1966**, *1*, 3.
- (18) Jørgensen, C. K. *Struct. Bonding* **1969**, *6*, 94.
- (19) Neese, F.; Solomon, E. I. *Inorg. Chem.* **1998**, *37*, 6568–6582.

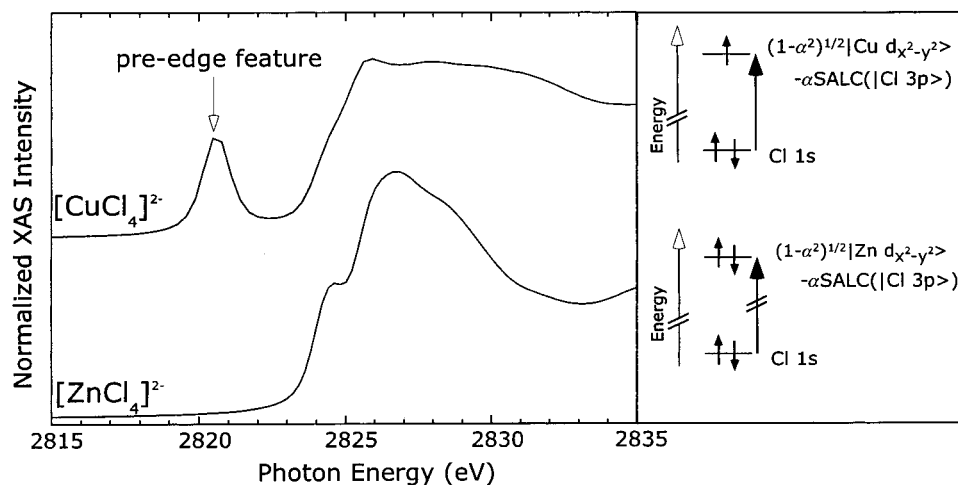


Figure 1. The principal ligand K-edge XAS experiment and illustrative experimental data for $[\text{CuCl}_4]^{2-}$ and $[\text{ZnCl}_4]^{2-}$ (adapted from ref 30).

certain extent arbitrary. An important exception is Bader's theory of atoms in molecules which introduces strictly defined atomic regions with definite quantum mechanical properties.²⁰ However, this is a small price to pay for the insight obtained from comparing experimental covalency numbers among series of related compounds.

Computationally the reliable calculation of the metal–ligand orbital mixing ratios is a difficult task. The Hartree–Fock method strongly overemphasizes the importance of the (large) exchange contribution to the electron–electron repulsion energy relative to the Coulomb part and is therefore biased in favor of high-spin states,^{21–23} low d-orbital occupations, and ionic bonds, and this is not corrected unless very extensive correlation treatments are employed.²⁴ Approximate density functional methods on the other hand are known to overestimate correlation and underestimate exchange effects. Consequently the bias is in favor of low spin states, high d occupations, and covalent bonds.²⁴ It might not be surprising in view of these facts that the more recently developed hybrid density functional methods^{25–27} that involve some of the Hartree–Fock exchange seem to perform best for open-shell transition metal complexes. However, given the difficulty in calculating highly reliable numbers, it is an especially important problem to have good experimental methods at hand that can give insight into the actual covalencies of metal–ligand bonds.

Previously, we have established that X-ray absorption (XAS) spectra of transition metal complexes with partly filled d shells display intense pre-edge features in the region of the ligand K-edge that can be attributed to transitions from ligand 1s core electrons into delocalized MOs that are shared between the metal and the ligands.^{28,29} This is demonstrated in Figure 1 where the Cl K-edge XAS spectra of $[\text{CuCl}_4]^{2-}$ and $[\text{ZnCl}_4]^{2-}$ are

compared.^{28,30} It is evident that only the Cu(II) complex displays the intense pre-edge feature that must therefore be related to a transition from the chlorine 1s orbital to the delocalized metal-based $d_{x^2-y^2}$ MO. The intensity of these transitions (normalized to unit edge jump) reflects the amount of ligand character mixed into the primarily metal-based partially occupied MOs and is therefore a direct measure of covalency as expressed in eq 1,²⁸

$$I(1s \rightarrow \psi^*) = a\alpha^2 \quad (1)$$

where α^2 is the amount of ligand character in the half-occupied copper-based MO and a is an empirical constant. In this way, the technique gives information comparable to EPR superhyperfine splittings but does not require the compound to be paramagnetic. In ref 29, the idea was further exploited that the pre-edge transition involves formally a charge transfer from a deep-lying ligand-based orbital to the metal. Since CT transitions are well-known to be proportional to the square of the metal–ligand distance,⁹ eq 1 has been modified to^{31,32} These equations

$$I(1s \rightarrow \psi^*) = a'R_{\text{ML}}^2\alpha^2 \quad (2)$$

hold for a single hole in the metal 3d shell, as is the case for copper complexes. In the general case, however, it is necessary to properly analyze the multiplet splittings that arise from the ligand ($1s^1$)–metal (d^{n+1}) configuration to obtain a total intensity that is a weighted sum of contributions of the form of eq 1 or 2.²⁹ The well-studied $[\text{CuCl}_4]^{2-}$ complex⁹ has served as a calibration standard for a or a' in (1) and (2) for studies at the Cl K-edge.^{28,29} For sulfur a or a' values were determined from the S K-edge spectra of the blue copper protein plastocyanin and the copper thiolate model complex Cu-tet-b.³¹ The studies were then extended to nitrite reductase,³³ the mixed-valence

- (20) Bader, R. F. W. *Atoms in Molecules—A Quantum Theory*; Clarendon Press: Oxford, England, 1990.
 (21) Hay, P. J. *J. Am. Chem. Soc.* **1978**, *100*, 2411.
 (22) Sasaki, S.; Aizawa, T.; Koga, N.; Morokuma, K.; Ohkubo, K. *Inorg. Chem.* **1989**, *28*, 103.
 (23) Veillard, A. *Chem. Rev.* **1991**, *91*, 743.
 (24) Bauschlicher, C. W. In *Encyclopedia of Computational Chemistry*; Schleyer, P. v. R., Ed. John Wiley and Sons Ltd.: Chichester, England, 1998; p 3084.
 (25) Becke, A. D. *Phys. Rev. A* **1988**, *38*, 3098.
 (26) Becke, A. D. *J. Chem. Phys.* **1993**, *98*, 1372.
 (27) Becke, A. D. *J. Chem. Phys.* **1993**, *98*, 5648.
 (28) Shadle, S. E.; Hedman, B.; Hodgson, K. O.; Solomon, E. I. *Inorg. Chem.* **1994**, *33*, 4235.
 (29) Shadle, S. E.; Hedman, B.; Hodgson, K. O.; Solomon, E. I. *J. Am. Chem. Soc.* **1995**, *117*, 7.

- (30) Hedman, B.; Hodgson, K. O.; Solomon, E. I. *J. Am. Chem. Soc.* **1990**, *112*, 1643.
 (31) Shadle, S. E.; Penner-Hahn, J. E.; Schugar, H. J.; Hedman, B.; Hodgson, K. O.; Solomon, E. I. *J. Am. Chem. Soc.* **1993**, *115*, 767.
 (32) Rose, K.; Shadle, S. E.; Eidsness, M. K., Jr.; Scott, R. A.; Hedman, B.; Hodgson, K. O.; Solomon, E. I. *J. Am. Chem. Soc.* **1998**, *120*, 10743.
 (33) LaCroix, L. B.; Shadle, S. E.; Wang, Y.; Averill, B. A.; Hedman, B.; Hodgson, K. O.; Solomon, E. I. *J. Am. Chem. Soc.* **1996**, *118*, 7755.
 (34) Williams, K. R.; Gamelin, D. R.; LaCroix, L. B.; Houser, R. P.; Tolman, W. B.; Moulder, T. C.; DeVries, S.; Hedman, B.; Hodgson, K. O.; Solomon, E. I. *J. Am. Chem. Soc.* **1996**, *119*, 2101.
 (35) Izumi, Y.; Glaser, T.; Rose, K.; McMaster, J.; Basu, P.; Enemark, J. H.; Hedman, B.; Hodgson, K. O.; Solomon, E. I. *J. Am. Chem. Soc.*, in press.

dicopper site Cu_A ,³⁴ and bis(oxo) Mo complexes.³⁵ More recently, the method was shown to be extremely useful in the field of monomeric,³² dimeric,³⁶ and tetrameric³⁷ iron–sulfur electron transfer centers. In all of these studies, key insight into the physical properties and the biological functions of these metal sites has been obtained.

The relationships among magnetic resonance parameters, spin densities, and covalent bonding are well-known and are being extensively used.^{19,38–43} However, less work has been done on ligand K-edge XAS. In this work we give a quantitative account of the intensities of the pre-edge transitions especially with respect to the analogy of ligand K-edge and CT transitions. We also report ab initio numerical investigations of the order of magnitude of the various terms appearing in the intensity expressions and how these change with the effective charge on the ligand.

Theory

Intensity Equation. The point of this study will be illustrated by taking a system with a single hole (i.e., a copper complex) as an example. The generalization to multiple-hole systems is then straightforward using the methods developed by Shadle et al.²⁹ The starting point is the frozen-orbital approximation to the initial and final states. The initial state is a single Slater determinant

$$|I\rangle = |\psi_1\bar{\psi}_1\cdots\psi_k\bar{\psi}_k\cdots\psi_n\bar{\psi}_n\psi_{\text{SOMO}}| \quad (3)$$

and the final state is the one where an electron is promoted from a ligand orbital with 1s character, ψ_k , to the SOMO

$$|F_k\rangle = |\psi_1\bar{\psi}_1\cdots\psi_k\bar{\psi}_{\text{SOMO}}\cdots\psi_n\bar{\psi}_n\psi_{\text{SOMO}}| \quad (4)$$

In the dipole length approximation to the transition dipole operator and with use of the Fermi golden rule, an electric dipole transition has intensity proportional to⁴⁴

$$D_k \propto |\langle F_k | \sum_A Z_A \bar{R}_A - \sum_i \bar{r}_i | I \rangle|^2 \propto |\langle \psi_{\text{SOMO}} | \bar{r} | \psi_k \rangle|^2 \quad (5)$$

where A sums over nuclei and i over electrons and Z_A is the nuclear charge of atom A . \bar{R}_A is the position of the A th nucleus, and \bar{r}_i and \bar{r} denote electron positions. If the Slater determinants were written in a spin-polarized scheme, the same equation would apply with the respective spin-down MOs substituting for ψ_{SOMO} and ψ_k . The ground-state singly occupied orbital, ψ_{SOMO} , is written

$$\psi_{\text{SOMO}} = \sqrt{1 - \alpha^2} |M\rangle - \alpha |L\rangle \quad (6)$$

where the overlap between the metal-centered part of the SOMO, $|M\rangle$, and the ligand-centered part, $|L\rangle$, is neglected. Therefore $100\alpha^2$ is the percentage ligand character in the SOMO which is distributed over the individual ligands that contribute

to the SOMO and $100(1 - \alpha^2)$ is the percentage metal character in the SOMO. The ligand part will, in general, be a linear combination of individual ligand orbitals:

$$|L\rangle = \sum_q c_{q,\text{SOMO}} |L_q\rangle \quad (7)$$

where q sums over the ligands and each individual ligand contribution is assumed to be a linear combination of valence ns and np orbitals

$$|L_q\rangle = \kappa_{q,\text{SOMO}} |ns\rangle + \sqrt{1 - \kappa_{q,\text{SOMO}}^2} |np\rangle \quad (8)$$

with hybridization coefficients $\kappa_{q,\text{SOMO}}$. The donor MO, ψ_k , is assumed to be a symmetry-adapted linear combination of only ligand 1s orbitals:

$$\psi_k = \sum_q b_{qk} |1s_q\rangle \quad (9)$$

The coordinate system is chosen so that the metal center lies at the origin. The final result will not, however, depend on this choice. The transition dipole matrix element becomes:

$$\begin{aligned} \langle \psi_{\text{SOMO}} | \bar{r} | \psi_k \rangle &= \langle \sqrt{1 - \alpha^2} |M\rangle - \\ &\alpha \sum_q c_{q,\text{SOMO}} \langle L_q | \bar{r} | \sum_q b_{qk} |1s_q\rangle \rangle = \\ &\sqrt{1 - \alpha^2} \sum_q b_{qk} \langle M | \bar{r} | 1s_q \rangle - \alpha \sum_q \sum_r c_{q,\text{SOMO}} b_{rk} \langle L_q | \bar{r} | 1s_r \rangle \end{aligned} \quad (10)$$

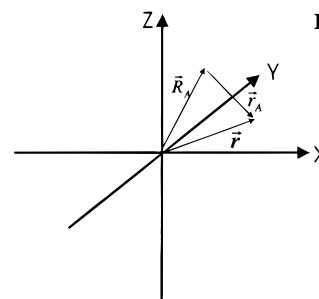
The first integral is in more detail

$$\langle M | \bar{r} | 1s_q \rangle = \int \phi_M(\bar{r} - \bar{R}_M) \bar{r} \phi_q(\bar{r} - \bar{R}_q) d^3\bar{r} \quad (11)$$

where the ϕ 's are the metal- and ligand-centered parts, respectively ($d^3\bar{r}$ is an infinitesimal three-dimensional volume element). It is convenient to note that

$$\bar{r} = \bar{R}_A + \bar{r}_A \quad (12)$$

where \bar{R}_A is any suitably chosen point and \bar{r}_A is the vector that points from \bar{R}_A to \bar{r} (see diagram I). Choosing, for example, \bar{R}_A



$= \bar{R}_M$, the integral is equal to

$$\begin{aligned} &\int \phi_M(\bar{R}_M + \bar{r}_M - \bar{R}_M) \{ \bar{R}_M + \bar{r}_M \} \phi_L(\bar{R}_M + \bar{r}_M - \\ &\bar{R}_q) d^3\bar{r}_M = \bar{R}_M \int \phi_M(\bar{r}_M) \phi_L(\bar{r}_M + \bar{R}_M - \bar{R}_q) d^3\bar{r}_M + \\ &\int \phi_M(\bar{r}_M) \{ \bar{r}_M \} \phi_L(\bar{r}_M + \bar{R}_M - \bar{R}_q) d^3\bar{r}_M \end{aligned} \quad (13)$$

The first integral is just an overlap integral between a metal-centered orbital and a ligand 1s orbital. The second integral is

(36) Rose, K.; Shadle, S. E.; Glaser, T.; DeVries, S.; Cherepanov, A.; Canters, G. W.; Hedman, B.; Hodgson, K. O.; Solomon, E. I. *J. Am. Chem. Soc.* **1999**, *121*, 2353.

(37) Glaser, T.; Rose, K.; Hedman, B.; Hodgson, K. O.; Solomon, E. I. Manuscript in preparation.

(38) Maki, A. H.; McGarvey, B. R. *J. Chem. Phys.* **1958**, *29*, 29, 34.

(39) McGarvey, B. R. *Transition Met. Chem* **1966**, *3*, 89.

(40) Kivelson, D.; Neimann, R. *J. Chem. Phys.* **1961**, *35*, 149.

(41) Keijzers, C. P.; DeBoer, E. *J. Chem. Phys.* **1972**, *57*, 1277.

(42) Smith, D. W. *J. Chem. Soc. A* **1970**, 3108.

(43) Stone, A. J. *Proc. R. Soc. London* **1963**, 424.

(44) Avery, J. B. *The quantum theory of atoms, molecules and photons*; McGraw-Hill: London, 1972.

Table 1. Representative Two-Center Overlap and Dipole Integrals (in bohr) between Copper 3d and Chlorine and Sulfur 1s Orbitals^a

| <i>R</i> (Å) | sulfur | | | | chlorine | | | |
|--------------|---------------------------|----------------------------------|---------------------------------|--|---------------------------|----------------------------------|---------------------------------|--|
| | $\langle z^2 1s\rangle^b$ | $\langle z^2 z_{Cu} 1s\rangle^b$ | $\langle x^2 - y^2 1s\rangle^c$ | $\langle x^2 - y^2 x_{Cu} 1s\rangle^c$ | $\langle z^2 1s\rangle^b$ | $\langle z^2 z_{Cu} 1s\rangle^b$ | $\langle x^2 - y^2 1s\rangle^c$ | $\langle x^2 - y^2 x_{Cu} 1s\rangle^c$ |
| 2.00 | 6.398 | 9.602 | 5.541 | 8.323 | 8.738 | 5.818 | 5.038 | 7.574 |
| 2.05 | 5.181 | 7.971 | 4.487 | 6.909 | 7.253 | 4.710 | 4.079 | 6.286 |
| 2.10 | 4.190 | 6.605 | 3.629 | 5.724 | 6.010 | 3.809 | 3.299 | 5.208 |
| 2.15 | 3.385 | 5.434 | 2.932 | 4.734 | 4.971 | 3.077 | 2.665 | 4.307 |
| 2.20 | 2.732 | 4.512 | 2.366 | 3.909 | 4.104 | 2.483 | 2.150 | 3.556 |
| 2.25 | 2.202 | 3.720 | 1.907 | 3.223 | 3.384 | 2.001 | 1.733 | 2.931 |
| 2.30 | 1.773 | 3.063 | 1.535 | 2.653 | 2.785 | 1.611 | 1.395 | 2.413 |
| 2.35 | 1.426 | 2.517 | 1.235 | 2.181 | 2.289 | 1.296 | 1.122 | 1.983 |

^a Numbers are to be multiplied by 10^{-4} . The copper 3d orbital was represented by the double- ζ contraction of Clementi and Roetti,⁵³ and the sulfur and chlorine 1s orbitals were represented by single- ζ functions with Clementi's exponents 15.54090 (S) and 16.5239 (Cl), respectively.⁵²

^b The ligand is positioned on the positive z axis. ^c The ligand is positioned on the positive x axis.

a two-center electric dipole integral. Representative values for these integrals are collected in Table 1. At typical bond distances (≈ 2.25 Å), the values for the largest of these integrals are on the order of 3×10^{-4} bohr. This is at least 1 order of magnitude smaller than the one-center terms (0.008–0.012 bohr; vide infra) to be discussed below. Therefore one can neglect the two-center integrals to a first approximation.

The majority of the intensity must therefore come from the second term in eq 10. Writing the integrals out in full, we have

$$\langle L_q|\vec{r}|1s_r\rangle = \int \phi_{L_q}(\vec{r} - \vec{R}_q)\{\vec{r}\}\phi_r(\vec{r} - \vec{R}_r) d^3\vec{r}_M \quad (14)$$

It is convenient to choose $\vec{R}_A = \vec{R}_q$ and therefore

$$\begin{aligned} \langle L_q|\vec{r}|1s_r\rangle &= \int \phi_{L_q}(\vec{r}_q)\{\vec{R}_q + \vec{r}_q\}\phi_r(\vec{r}_q + \vec{R}_q - \vec{R}_r) d^3\vec{r}_q = \\ &\vec{R}_q \int \phi_{L_q}(\vec{r}_q)\phi_r(\vec{r}_q + \vec{R}_q - \vec{R}_r) d^3\vec{r}_q + \\ &\int \phi_{L_q}(\vec{r}_q)\{\vec{r}_q\}\phi_r(\vec{r}_q + \vec{R}_q - \vec{R}_r) d^3\vec{r}_q \quad (15) \end{aligned}$$

If $q \neq r$ (functions on different ligands), the first integral is the overlap of a valence orbital on one ligand with the 1s orbital of another ligand and must be very small. Again the second term is a two-center dipole integral and is of the same order of magnitude than the overlap integral and can also be neglected.

This leaves only one contribution to the intensity, which arises from two functions that are centered on the same ligand ($q = r$). Thus, the integral is of the form

$$\langle L_q|\vec{r}|1s_q\rangle = \vec{R}_q \int \phi_{L_q}(\vec{r}_q)\phi_q(\vec{r}_q) d^3\vec{r}_q + \int \phi_{L_q}(\vec{r}_q)\{\vec{r}_q\}\phi_q(\vec{r}_q) d^3\vec{r}_q \quad (16)$$

Substituting the explicit forms, we have

$$\begin{aligned} \langle L_q|\vec{r}|1s_q\rangle &= \vec{R}_q \int (\kappa_{q,\text{SOMO}}\phi_{ns_q}(\vec{r}_q) + \\ &\sqrt{1 - \kappa_{q,\text{SOMO}}^2}\phi_{np_q}(\vec{r}_q))\phi_{1s}(\vec{r}_q) d^3\vec{r}_q + \int (\kappa_{q,\text{SOMO}}\phi_{ns_q}(\vec{r}_q) + \\ &\sqrt{1 - \kappa_{q,\text{SOMO}}^2}\phi_{np_q}(\vec{r}_q))\{\vec{r}_q\}\phi_{1s}(\vec{r}_q) d^3\vec{r}_q \quad (17) \end{aligned}$$

The first integral is a one-center core-valence overlap and by construction vanishes. For the second integral, the electric dipole selection rules demand that only the p-part of the ligand function be active. The integral is a one-center electric dipole integral and is readily evaluated. Finally

$$\langle L_q|\vec{r}|1s_q\rangle = \sqrt{\frac{1 - \kappa_{q,\text{SOMO}}^2}{3}} \langle r \rangle_{np_q,1s_q} \vec{e}_{p_q} \quad (18)$$

where \vec{e}_{p_q} is a unit vector that has the same direction as the p orbital on ligand q that contributes to the SOMO and the factor $3^{-1/2}$ derives from the angular part of the integral. The radial integral in eq 18 is defined as

$$\langle r \rangle_{np_q,1s_q} = \langle \text{Rad}_{np_q} | r | \text{Rad}_{1s_q} \rangle \quad (19)$$

where “Rad” denotes the radial part of the orbitals. Thus, the final expression for the transition dipole matrix elements becomes to a good approximation

$$\langle \psi_{\text{SOMO}} | \vec{r} | \psi_k \rangle = -\alpha \sum_q c_{q,\text{SOMO}} b_{qk} \sqrt{\frac{1 - \kappa_{q,\text{SOMO}}^2}{3}} \langle r \rangle_{np_q,1s_q} \vec{e}_{p_q} \quad (20)$$

The c 's are merely the coefficients required for the symmetry-adapted linear combinations of ligand orbitals. The simplest case is met when there is only one ligand that contributes to the ligand K-edge intensity. The square of the transition dipole moment is (dropping the label q)

$$|\langle \psi_{\text{SOMO}} | \vec{r} | \psi_k \rangle|^2 = 1/3 \alpha^2 c_{\text{SOMO}}^2 (1 - \kappa_{\text{SOMO}}^2) \langle r \rangle_{np,1s}^2 \quad (21)$$

The expression has a straightforward interpretation—the pre-edge intensity increases as the ligand character the SOMO increases (α^2), as the ligand in question makes a larger contribution to the total ligand character in the SOMO (c_{SOMO}^2) and as the p character of this contribution increases ($1 - \kappa_{\text{SOMO}}^2$). In absolute terms, for a particular ligand atom, the factor $1/3 \langle r \rangle_{np,1s}^2$ is the intrinsic intensity of an atomic $1s \rightarrow np_{x,y,z}$ transition.

Comparison to Charge Transfer Transitions. It is interesting to compare the situation for a ligand K-edge transition with that for a charge transfer transition in the visible region of the spectrum. The situation for a typical CT is analyzed in Figure 2. The donor orbital is mainly localized on the ligand and is bonding with the metal. It is thus of the following form:

$$\psi_{\text{donor}} = \alpha |M\rangle + \sqrt{1 - \alpha^2} |L\rangle \quad (22)$$

For illustrative purposes, the same metal and ligand parts are assumed in the SOMO and the donor MO; such “bonding to antibonding transitions” will generally have the highest intensities among the possible ligand-to-metal CT transitions. This gives for the transition dipole moment

$$\langle \psi_{\text{SOMO}} | \vec{r} | \psi_{\text{donor}} \rangle = \alpha \sqrt{1 - \alpha^2} (\langle M | \vec{r} | M \rangle - \langle L | \vec{r} | L \rangle) + (1 - 2\alpha^2) \langle M | \vec{r} | L \rangle \quad (23)$$

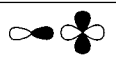
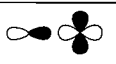

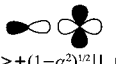


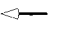
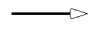
| | Ligand K-edge L—M | Charge-Transfer L—M |
|--------------------------|--|--|
| Acceptor MO |  $(1-\alpha^2)^{1/2} M\ 3d\rangle - \alpha L\ np\rangle$ |  $(1-\alpha^2)^{1/2} M\ 3d\rangle - \alpha L\ np\rangle$ |
| Donor MO |  $ L\ 1s\rangle$ |  $\alpha M\ 3d\rangle + (1-\alpha^2)^{1/2} L\ np\rangle$ |
| Transition Density |  |  |
| Transition Dipole Moment |  $\alpha\langle 1s x np\rangle$ |  $\alpha(1-\alpha^2)^{1/2}R$ |

Figure 2. Comparison of the electric dipole intensity mechanisms for ligand K-edge transitions and optical charge transfer transitions.

Using eq 12

$$\langle M|\vec{r}|M\rangle = \langle M|\vec{R}_M + \vec{r}_M|M\rangle \approx \vec{R}_M \quad (24a)$$

$$\begin{aligned} \langle L|\vec{r}|L\rangle &= \sum_{p,q} c_{p,SOMO} c_{q,donor} (\langle L_p|\vec{R}_q + \vec{r}_q|L_q\rangle) \approx \\ &\sum_q c_{q,SOMO} c_{q,donor} (\vec{R}_q + \{\kappa_{q,SOMO} \sqrt{1 - \kappa_{q,donor}^2} + \\ &\kappa_{q,donor} \sqrt{1 - \kappa_{q,SOMO}^2}\} \langle ns_q|\vec{r}_q|np_q\rangle) \quad (24b) \end{aligned}$$

In the first term (eq 24a), contributions due to possible d–p hybridization contributions on the metal are neglected, and in the second term (eq 24b), the two-center integrals between different ligands are neglected. The final term in eq 23, which consists of only two-center terms, is neglected for the qualitative discussion. Finally the transition dipole moment for the bonding-antibonding CT transition is approximately given by

$$\langle \psi_{SOMO}|\vec{r}|\psi_{donor}\rangle = \alpha \sqrt{1 - \alpha^2} (\vec{R}_M - \sum_q \vec{R}_q + h_q \langle ns_q|\vec{r}_q|np_q\rangle) \quad (25)$$

where h_q describes the combination of hybridization coefficients κ in eq 24b. There are two main contributions to the transition moment. The last term on the right is a local contribution and arises from the s–p hybridization on the ligand. It reflects an intraatomic $ns \rightarrow np$ transition and is therefore weighted with the transition dipole matrix element for such a transition. The second, more important, part is proportional to the metal–ligand distance ($|\vec{R}_M - \vec{R}_q|$). This contribution describes the shift of electron density from the ligand to the metal upon CT excitation. Such a contribution is not present in the ligand K-edge intensity expression, eq 20, because in this case, the donor MO is completely localized on the ligand. These relationships are illustrated in Figure 2. For a ligand-to-metal CT transition, the transition density contains a dominant contribution proportional to the metal–ligand distance, because both the donor and the acceptor MO are shared between the metal and the ligand, which introduces a large transition dipole moment along the metal–ligand bond. Alternatively, in a ligand K-edge transition, the donor MO is entirely localized on the ligand, which makes the transition density on the metal vanishingly small and leaves only the contributions due to the local dipole moment on the ligand.

Charge Dependence of Transition Dipole Moment Integrals. As is evident from the discussion above, the intensity of

a given pre-edge transition is determined predominantly by the amount of ligand 3p character in the partially occupied orbitals weighted by the transition dipole integral for the “quasi-atomic” $1s \rightarrow 3p$ transition. The value of this integral depends on the radial functions of the ligand 1s and 3p orbitals, which will in turn depend on the effective valence shell population and the effective nuclear charge of the ligand. To determine how the value of this integral depends on the charge on the ligand, Hartree–Fock calculations were carried out on free ions of sulfur and chlorine as described under Computational Details. The results of these calculations are shown in Figure 3. As the number of p electrons increases, the valence 3p orbital becomes more diffuse, as evidenced by the increase in the expectation value $\langle r \rangle_{3p}$ shown in Figure 3C,D. At the same time the dipole integral $\langle 1s|x|3p_x \rangle$ decreases because the 3p orbital has its concentration of charge more distant from the very compact 1s orbital. However, as can be seen from the results in Figure 3, the charge dependence of the integrals $\langle 1s|x|3p_x \rangle$ is quite modest. Translated to the molecular case, an increase in the effective chlorine 3p population from 5.22 to 5.69 only causes the value of the integral to change by some 3%. The changes for sulfur are somewhat more pronounced—for the same change in population, the integral varies by 5–6%. Sulfur can also be expected to have a stronger variation in its effective 3p population than chlorine in actual molecules due to the existence of multiple bonding modes (for example, $\mu_2\text{-S}^{2-}$, $\mu_3\text{-S}^{2-}$, R–S[–], and R–S–R). To conclude this paragraph, it is noted that, given a reasonable MO calculation for the reference molecule and using the interpolation formulas shown in Figure 3, the charge dependence of the transition dipole integral can be taken into account by scaling the experimental intensity as in eq 26,

$$I' = \frac{I^{\text{mol}} \langle r \rangle_{1s,3p}^{\text{ref}} (N_{3p}^{\text{ref}})}{I^{\text{ref}} \langle r \rangle_{1s,3p}^{\text{mol}} (N_{3p}^{\text{mol}})} \quad (26)$$

where I' is the corrected relative experimental intensity, I^{mol} is the pre-edge intensity of the molecule under investigation, I^{ref} is the pre-edge intensity of the reference molecule, $\langle r \rangle_{1s,3p}^{\text{ref}} (N_{3p}^{\text{ref}})$ is the transition dipole integral of the reference molecule using the calculated 3p population (N_{3p}^{ref}), and $\langle r \rangle_{1s,3p}^{\text{mol}} (N_{3p}^{\text{mol}})$ is the transition dipole integral of the molecule under investigation using the 3p population calculated with the same theoretical method as the standard. However, the changes in covalency numbers caused by this correction will be quite small.

Electronic Relaxation. Change in the shapes of MOs upon creation of core holes is an important aspect of high-energy electron and X-ray spectroscopy. For the case of ligand K-edge transitions, the final state produces a hole in a ligand 1s orbital. Thus, the valence electrons on that ligand are less shielded from the nuclear charge of the ligand and will therefore stabilize upon excitation. Since the electronic relaxation will work in a direction to minimize the energy of the core hole, it can only be effective if low-lying empty orbitals become significantly populated due to the relaxation process. However, chlorine- and sulfur-containing ligands are typical π -donor ligands which do not have low-lying empty orbitals available to provide efficient relaxation pathways. In fact, the first available unoccupied orbitals in a prototypical copper complex with donor ligands are the metal 4s and 4p orbitals. These are known to be significantly more diffuse than the 3d orbitals such that they can have significant amplitude at the position of the ligand nuclei. Thus an increase in their population in the final state could provide electron density that stabilizes the core hole.

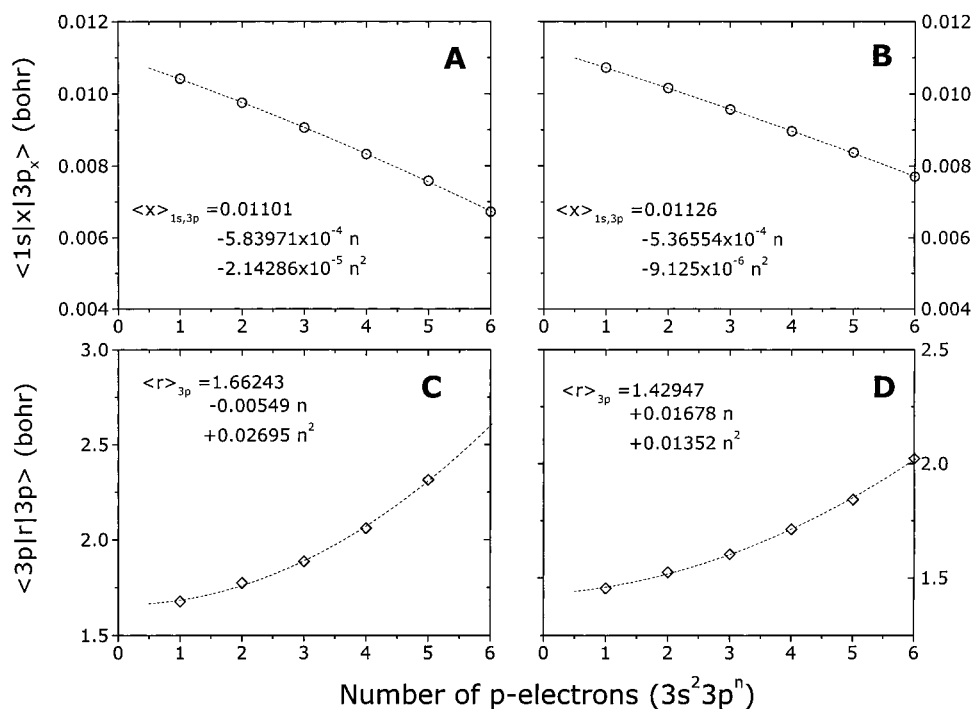


Figure 3. Charge dependence of the transition dipole integrals $\langle x \rangle_{1s,3p}$ for sulfur (A) and chlorine (B) in their $3s^2 3p^n$ configurations as calculated by spin-averaged Hartree–Fock calculations. Panels C and D plot the radial expectation value of the sulfur (C) and chlorine (D) 3p orbitals. The dashed lines are second-order polynomial fits with the coefficients given in each panel.

However, because the final state is characterized by a d^{n+1} configuration on the metal, the metal 3d, 4s and 4p orbitals will all rise in energy due to the increased interelectronic repulsion on the metal. The 4s and 4p orbitals may therefore not be as effective in providing relaxation pathways as unoccupied ligand-based orbitals.

Hartree–Fock calculations were carried out on the prototypical complex $[\text{CuCl}_4]^{2-}$ as described under Computational Details to evaluate the factors on a more quantitative level. Three calculations were carried out on (a) the ground state, (b) an averaged unrelaxed core-hole state in which one electron has been promoted from the four ligand 1s orbitals to the SOMO, and (c) an averaged relaxed core-hole state in which the average of the four $1s \rightarrow \text{SOMO}$ states was reconverged.⁴⁵ The relaxation energy upon reconverging to the core-hole state is surprisingly small and amounts to only ≈ 2 eV (Table 2). The absolute energy calculated for the pre-edge transition is 2844 eV, which deviates by ≈ 24 eV from the experimental value.²⁸ The discrepancy is attributed to correlation and relativistic effects that would require a more detailed treatment which is outside the scope of this study. The orbital populations show that, without relaxation, the Cu 3d population increases by almost one electron, as expected, whereas the change in Cu 4s and 4p population is negligible (Table 2). Upon reconverging, some charge flows back from the copper to the ligands, as evidenced by a decrease in both the Cu 3d and Cu 4s,p populations, which is also expected on the basis of the considerations in the previous paragraph. However, the changes in populations upon recon-

Table 2. Mulliken Orbital Populations of $[\text{CuCl}_4]^{2-}$ for the Initial State, Unrelaxed Core-Hole State, and Relaxed Core-Hole State from Hartree–Fock Calculations^a

| | initial state | changes relative to initial state | |
|-----------------------|---------------|-----------------------------------|-------------------|
| | | unrelaxed core hole | relaxed core hole |
| Cu 3d | 9.233 | 0.918 | 0.723 |
| Cu 4s | 0.224 | 0.000 | -0.111 |
| Cu 4p | 0.360 | 0.001 | -0.168 |
| E_{tot} (eV) | -94 478.77 | 2846.2 | 2844.5 |

^a The unrelaxed core hole was obtained by redistributing electrons from the ground state to the average core-hole configuration $\frac{1}{2}(|\text{Cl}_A 1s \rightarrow \text{SOMO}| + |\text{Cl}_B 1s \rightarrow \text{SOMO}| + |\text{Cl}_C 1s \rightarrow \text{SOMO}| + |\text{Cl}_D 1s \rightarrow \text{SOMO}|)$. The relaxed core hole was obtained by reconverging the calculation to this state.

verging the calculation are not very large. It is also noted that the population of the Cl 3d orbitals is negligible in all calculations and that the MOs describing the core hole are almost purely Cl 1s in character.

In summary, these calculations support the idea that electronic relaxation effects are relatively small in ligand K-edge transitions and help to rationalize the lack of experimental evidence for shake-up satellite peaks which would reflect final state changes. Such effects are expected to be more prominent if low-lying empty orbitals on the ligand are available, which is not the case for the predominantly π -donor Cl- and S-based ligands.

Discussion

In conclusion, the intensity mechanism for ligand K-edge transitions relative to charge transfer transitions was studied. As noted previously,^{28,29,31} the method is a highly useful probe of metal–ligand covalency because the pre-edge intensity is directly proportional to the amount of p character in the partially occupied acceptor MOs. However, there is no metal–ligand distance factor in the expressions for the intensity of a ligand K-edge transition. Instead, there is the value for the intensity of an intrinsic “quasi-atomic” intraligand $1s \rightarrow np$ transition which arises because the transition is localized on the

(45) In many studies, the molecular symmetry is broken for core to valence excitations in order to circumvent problems of the Hartree–Fock approximation in treating core-hole states correctly. Such broken-symmetry states yield better energies but wave functions of questionable physical content. In this study, we are interested not in the calculation of energies but rather in the calculation of intensities. The total pre-edge intensity obtained from summing over all four individual Cl 1s to SOMO transitions, which are at the same energy because the Cl 1s orbitals are virtually noninteracting, equals 4 times the intensity of a localized Cl 1s to SOMO excitation.

ligand(s). Thus, the analogy between charge transfer and ligand K-edge transitions is purely formal and does not extend to the interpretation of the dominant intensity mechanisms. If the open-shell structure of the complex is more complicated, so that there are multiplet effects, the situation is still the same, only that the intensities need to be weighted with suitable coefficients that result from vector-coupling operations as described previously.^{29,46}

The absolute values of the integrals $\langle 1s|r|np \rangle$ are quite small because the effective length of electron oscillation is very short; i.e., it is of the order of the spatial extent of the ligand 1s orbitals (≈ 0.1 bohr). Thus the absolute transition dipole moments of these transitions are much smaller than those of intense charge transfer transitions where the effective oscillation length is of the order of the metal ligand distance (≈ 4 bohr).

A further point concerns the charge dependence of the localized transition dipole moment integral $\langle 1s|r|np \rangle$. The calculations show that the dependence of this integral on the effective charge on the ligand is moderate. Thus, given reliable MO calculations for a suitable intensity standard and the molecule under investigation, the charge dependence can be approximately taken into account using Figure 3 but will not lead to a large correction on the experimentally determined covalency numbers. However, significant changes could be induced by the radial distortions that occur upon covalent bond formation.¹⁹ For example, in a recent study, it was shown that the intrinsic intensity of a ligand K-edge transition is 18% lower for a sulfide compared to a thiolate ligand.^{36,47} While this trend is in the direction predicted by the calculations, the change is larger than expected. This additional modification of the valence radial distribution functions may be caused by the effects of different bonding interactions in a thiolate versus a sulfide, especially the presence of the covalent C–S bond in a thiolate. A more detailed study is required to evaluate this point.

We have also studied two further factors that could affect the simplicity of the analysis. The first one is the presence of two-center integrals in the intensity expressions. These were found to be 1–2 orders of magnitude smaller than the one-center terms by direct evaluation.

The second point concerns the presence of electronic relaxation. In transition metal core level photoelectron spectra, relaxation effects appear as prominent shake-up satellites that originate from ligand-to-metal CT states that sharply drop in energy because the core hole on the metal stabilizes the unoccupied or partially occupied metal d orbitals.^{36,48–51} For ligand K-edge XAS spectra, an efficient relaxation pathway would have to utilize low-lying empty orbitals on the ligand to induce metal-to-ligand shake-up intensity. However, these are not available for the typical Cl- and S-based ligands that are predominantly π -donor in character. Alternatively the core hole on the ligand could be stabilized by an increase in the metal 4s,p populations because these orbitals are diffuse enough to

extend spatially onto the ligand. However, the final-state electron configuration is d^{n+1} on the metal which will destabilize the metal 3d and 4s,p orbitals and make them less available. Thus, these relaxation pathways can be expected to be inefficient, and this has been observed in the calculations reported in this study. The absence of extensive electronic relaxation is supported by the experimental lack of significant shake-up intensity.

In summary, the methodology developed previously^{28,29,46} for the analysis of ligand K-edge intensities in terms of covalent bonding appears to rest on a solid foundation and is a highly useful tool in the study of covalency effects in monomeric^{28,29,31,32,35} and oligomeric^{28,34,36,37} transition metal complexes where the results from lower energy spectroscopic methods can be less straightforward to interpret due to the complexity of the data.

Computational Details

All ab initio calculations reported in this paper were carried out with the program Orca developed by F.N. For the atomic Hartree–Fock calculations, Slater type orbitals (STOs) were used with exponents taken from Clementi and Raimondi.⁵² The valence-shell exponents consisted of two primitives taken from Clementi and Roetti⁵³ and three more primitives with exponents 0.3, 1.0, and 4.0 (4.5 for Cl). The calculations were converged to 10^{-8} eV. The spin-averaged Hartree–Fock method of Zerner and co-workers was used in all cases for the maximal total spin arising from a given configuration.^{54–56} The integrals in Table 1 were determined by direct analytical integration in elliptic coordinates.

The molecular Hartree–Fock calculations were also carried out with a basis set of STOs. This was made possible by the extensive development of integral algorithms by Fernandez-Rico, Lopez, and co-workers.^{57,58} However, all three- and four-center electron repulsion integrals were calculated with a six-term Gaussian expansion of the STOs. Since all large integrals are calculated exactly, this procedure produces negligible errors relative to the exact STO calculation.^{57,58} The basis set consisted of the Clementi–Raimondi exponents⁵² up to 2p (Cl) and 3p (Cu). For the valence shell, the two primitives of the double- ζ wave functions of Clementi and Roetti⁵³ were uncontracted. A third d shell with exponent 1.0 was added to the copper basis. The 4s and 4p orbitals of copper were each represented by two primitives with exponents taken from the 4s orbital reported by Clementi and Roetti.⁵³ In addition, a set of 4f polarization functions was added to the copper basis and a 3d shell with exponent 1.75 to the chlorine basis. For technical reasons, the geometry employed for square planar $[\text{CuCl}_4]^{2-}$ was slightly reduced to D_{2h} by choosing the bond lengths 2.249 and 2.251 Å.

Acknowledgment. Our research was supported by the National Science Foundation (Grants CHE-9528250 (E.I.S.) and CHE-9423181 (K.O.H.)) and the NIH (Grant RR-01209 (K.O.H.)). F.N. acknowledges a postdoctoral fellowship from the Deutsche Forschungsgemeinschaft. We thank Dr. Thorsten Glaser for useful discussions. Professors Fernandez-Rico and Lopez (University of Madrid, Spain) and their co-workers are gratefully acknowledged for generously supplying us with their STO integral program allowing the molecular ab initio STO calculations.

IC990461P

(46) Shadle, S. E. Ph.D. Thesis; Stanford University, 1994.

(47) Experimentally the spectra are normalized to the continuum oscillator strength. These states are unbound and therefore less sensitive to the molecular potential than the bound states. Chemical effects on the continuum are largely taken into account by referencing the pre-edge intensity to different types of ligand binding modes (i.e., thiolate versus sulfide).

(48) van der Laan, G. *Phys. Rev. B* **1981**, 23, 4369.

(49) Davis, L. C. *Phys. Rev. B* **1982**, 25, 2912.

(50) Park, J.; Ryu, S.; Han, M.; Oh, S. J. *Phys. Rev. B* **1988**, 37, 10867.

(51) Butcher, K. D.; Gebhard, M. M.; Solomon, E. I. *Inorg. Chem.* **1990**, 29, 2067.

(52) Clementi, E.; Raimondi, D. L. *J. Chem. Phys.* **1963**, 38, 2686.

(53) Clementi, E.; Roetti, C. *Atom. Nucl. Data Tab.* **1974**, 14, 177.

(54) Stavrev, K. K.; Zerner, M. C. *Int. J. Quantum Chem.* **1997**, 65, 877.

(55) Zerner, M. C. *Int. J. Quantum Chem.* **1989**, 35, 567.

(56) Edwards, W. D.; Zerner, M. C. *Theor. Chim. Acta* **1987**, 72, 347.

(57) Fernandez-Rico, J.; Lopez, R.; Ramirez, G. In *Structure, Interactions and Reactivity*; Fraga, S., Ed.; Elsevier: Amsterdam, 1992; Vol. 77 (A), p 241.

(58) Fernandez-Rico, J.; Lopez, R.; Aguado, A.; Ema, I.; Ramirez, G. *J. Comput. Chem.* **1998**, 19, 1284.